Proceedings of ASME Turbo Expo 2009: Power for Land, Sea and Air
GT2009
June 8-12, 2009, Orlando, Florida, USA

GT2009-60199

COMPUTATIONAL DESIGN OF A LOUVER PARTICLE SEPARATOR FOR GAS TURBINE ENGINES

Grant O. Musgrove
Michael D. Barringer
Karen A. Thole
The Pennsylvania State University
Mechanical and Nuclear Engineering Department
University Park, PA 16802

Eric Grover
Joseph Barker

United Technologies Corporation – Pratt & Whitney
400 Main Street
East Hartford, CT 06108

ABSTRACT

The extreme temperatures in a jet engine require the use of thermal barrier coatings and internal cooling channels to keep the components in the turbine section below their melting temperature. The presence of solid particles in the engine's gas path can erode thermal coatings and clog cooling channels, thereby reducing part life and engine performance. This study uses computational fluid dynamics to design the geometry of a static, inertial particle separator to remove small particles, such as sand, from the engine flow. The concept for the inertial separator includes the usage of a multiple louver array followed by a particle collector. The results of the study show a louver design can separate particles while not incurring large pressure loss.

NOMENCLATURE

A	louver anchor length
AR	area ratio, AR=δ(# Louvers)/H
AsR	aspect ratio of design space, AsR=X/H
C_D	particle drag coefficient
D_c	Stokes characteristic dimension
d_p	particle diameter
ΔP	pressure loss, $\Delta P=(P_{in}-P_{ex})_{total}/(P_{in})_{total}$
H	height of design space
L	louver length, L=δ/sinϕ
Re	inlet Reynolds number $Re=\rho H U_{in}/\mu$
Re_p	particle Reynolds number $Re_p=\rho d_p \lvert U_p-U \rvert/\mu$
Re_{sph}	particle Reynolds number using the dia. of a sphere with equivalent particle volume
s	surface area of a sphere with equivalent particle volume
S	surface area of the actual particle
U	local fluid velocity
U_p	local absolute particle velocity
w	distance between last louver tip and top domain wall
X	axial length of design space
Z	particle shape factor, Z=s/S

Greek

δ	louver gap, δ=AR·H/(# Louvers)
η	collection efficiency, $\eta=1-(N_{escaped}/N_{injected})_{particles}$
θ	louver axis angle , $\theta=\tan^{-1}(1/AsR)$
μ	fluid dynamic viscosity
ρ_f	fluid density
ρ_p	particle density
τ_{rea}	particle reaction time, $\tau_{res}=\rho_p d_p^2/18\mu$
τ_{res}	particle residence time, $\tau_{res}=D_c/U_p$
ϕ	louver angle with respect to θ

INTRODUCTION

Ingestion of solid particles into gas turbine engines occurs during takeoff, landing, and in flight. On the ground, helicopters stir up dust with their rotors that result in severe ingestion. Airplanes, on the other hand, create an intake vortex between the engine inlet and the ground that lifts debris and sand into the engine [1]. During flight, particles can be ingested when flying low in dusty environments, such as deserts, or when flying through volcanic ash clouds [2]. Ingested particles reduce the performance and life of an engine through surface erosion, deposition, and the blocking of cooling channels in the turbine. Cooling channel blockage is increased by particle size [3,4] and amount of particles [3,4,5] ingested.

While there are many particle separation methods, inertial separators are best applicable to aircraft engines because of their ability to handle high flow rates while not significantly increasing pressure losses in the engine. Two commonly applied inertial separators are cyclones and particle deflectors combined with some type of particle trap. Both types make use of inertial forces to separate particles from the fluid flow. Variations of the particle deflectors and cyclones have been applied to gas turbines [6-10] and are generally integrated into various locations within the engine. A deflector design that is often used in helicopters is integrated into the inlet of the engine and is known as an inlet particle separator. An inlet particle separator contains a secondary flow system (scavenge flow) that is separate from the engine flow. The scavenge flow convects particles away from the main gas path through a separate duct. Another common deflector is a louver design, which also uses a scavenge flow duct similar to the inlet particle separator, but the louver design has yet to be applied to aircraft engines. Neither the inlet particle separator nor louver separator designs have been applied in a location other than the inlet to gas turbines.

The particle separator concept presented in this paper is a louver separator, but is one that does not require a scavenge flow. The separator presented in this paper is one that uses a static collection bin (collector) to capture the separated particles, located downstream of a series of louvers. This particular separator concept is intended for placement within the combustor bypass flow. The particle separator is intended to remove particles that could potentially block cooling channels in the turbine section of the engine. This paper presents a computational study of a particle separator containing both a louver section and a collector section. The focus of the study is to minimize the pressure loss and maximize the particle collection. This study evaluates various louver arrays and collector geometries while maintaining a fixed channel size (design space) and set of flow boundary conditions. The remainder of the paper includes a brief presentation of relevant literature, explanation of the geometry and computational model of the separator concept, and presents particle collection and pressure loss results for various simulated geometry configurations.

REVIEW OF RELEVANT LITERATURE

Past literature indicates that inertial separators have potential for turbine applications to remove particles from engine flow. This section documents previous methods used for computationally modeling two-phase flow in particle separators. The summary of the literature also provides insights that helped guide the work completed in the current study.

Many of the studies presented in the literature have focused on inlet particle separators applied to helicopters. Breitman et al. [11] performed a numerical study, similar to Vittal et al. [12] and Shieh et al. [13], in which they found that large particles are more resistant than small particles to changes in flow trajectory due to their high inertia. Stokes theory states that at low Stokes numbers (small particle diameters) particles follow the fluid flow whereas at high Stokes numbers (large particle diameters) the particles do not follow the flow

Zedan et al. [14] expanded the work of others [11-13] to show computational agreement of overall particle separation with measurements for two distinct inlet particle separators. Zedan et al. reported particle collection efficiencies between 82-85%. Using a similar conceptual design and modeling approach, Ghenaiet and Tan [15] reported separation efficiencies greater than 80%, depending on sand size distribution and scavenge flow rates. Modifying the separator geometry to control the particle trajectories and surface impacts, Ghenaiet and Tan increased overall particle separation efficiency by almost 10%. Collection of small particles was increased by as much as 80%. Ghenaiet and Tan's analysis agreed with Breitman et al. in that the small particle trajectories are dominated by drag forces. Conversely, large particle trajectories are more resistive than small particles to changes in flow direction.

A number of investigators have evaluated design features associated with louver separators. These design features include the louver angle, louver length, louver spacing, louver overlap, scavenge flow rate, and Reynolds number. Past studies show effects of these design parameters on pressure losses and particle separation.

One of the earliest studies of a louver separator was performed by Zverev [16]. Separation efficiency was experimentally measured and found to increase with increased scavenge flow rate, increased Reynolds number, and decreased louver spacing. Zverev found that increasing the louver angle reduced the pressure loss of the separator. The highest particle separation occurred for a 30° louver angle. The trends in separation efficiency found by Zverev were experimentally confirmed for other louver separators by Smith and Goglia [17], Gee and Cole [18], and Poulton et al. [19].

Smith and Goglia [17] found that particle separation was highly dependent upon the location of the particle's impact on the louver. They found that separation efficiency could be increased by modifying the louver array to eliminate the louver overlap and to include a louver anchor. Furthermore, their work defined that equal flow rates through each louver passage was necessary for good collection efficiency, confirmed by Gee and Cole [18]. Smith and Goglia found that dust loading has little effect on particle collection, which was also confirmed experimentally by Gee and Cole [18]. Dust loading refers to the mass flow rate of particles relative to the flow stream. Gee and Cole showed that a V-shaped louver did not improve particle separation over a straight louver although V-shaped louvers reduced the pressure loss.

Poulton et al. [19] used flow visualization on a louver separator and found a significant separation region on the backside of the louvers. This region was found to affect the particle trajectories near the louvers by changing the radius of curvature of the flow around the louvers. The separation region also increased the pressure loss of the separator by reducing the effective flow area between the louvers. Poulton et al. found that pressure loss could be reduced by spacing the louvers such that the flow along the backside of the louver reattached to the louver. Additional experiments by Poulton et al. indicated that separation efficiency increased with louver

thickness and reduced louver spacing. The effect of Reynolds number on separation efficiency agreed with previous studies, but Poulton et al. showed that there is an upper limit. Pressure loss was reported to increase with louver length, and it was found that there is a favorable combination of louver overlap and louver spacing.

Past studies have modeled two-phase flow in inertial separators by first solving for the flow field in the separator, and then calculating particle trajectories by solving a force balance on each particle. This method assumes that the particle concentration in the fluid is small enough that particle-particle interactions are negligible. This method also assumes that there is no effect of the particles on the flow field. Methods for solving the flow field in the separator have included both ideal flow [11,12,18,19,20] and fully turbulent viscous models [14,15].

The force balance used to calculate a particle trajectory includes a drag force term. Most investigators [11,14,18-20] have used a modified form of the Stokes' drag coefficient on a sphere. To correct for the irregular shape of solid particles, Breitman et al. [11] and Zedan et al. [14] made use of empirical shape factor data to modify the drag force term. Particle shape factor is used to quantify how spherical a particle is. Shape factor ranges from a value of zero (a highly irregularly shaped particle) to a value of one (a perfectly shaped sphere).

Another important modeling consideration is the use of a particle restitution coefficient, which is the ratio of particle velocity after and before an impact. A value of one indicates that velocity magnitude is unchanged by the impact, and zero indicates the particle has no velocity after impact. Restitution coefficients can vary with impact angle and material. Previous studies [11,12,14,19] have found agreement with experimental results when using particle restitution coefficients. Breitman et al. [11] and Poulton et al. [19] used constant values for restitution coefficients, where Breitman found that using values of 1 and 0.85 for the tangential and normal restitution coefficients, respectively, improved agreement with experimental data.

Presented in this paper is a computational design of the louver-type separator using a two-dimensional model of the louver array and collector. The computational model includes the use of a k-ω turbulence model with enhanced wall functions for the near wall region. Collection efficiency and pressure loss results are presented for a number of design parameters including area ratio, louver angle, louver shape, number of louvers, and collector geometry. Unique about this study is that the evaluated louver separator uses a static collector instead of scavenge flow.

LOUVER SEPARATOR GEOMETRY AND DESIGN APPROACH

For this particular application, a louver separator with a fixed design space is considered for use in an aircraft gas turbine. The intended location of the separator is downstream of the combustor, as shown in Figure 1, along the outer casing of the first stage turbine. Here, the particle separator is intended to remove particles from the engine's bypass flow before the bypass flow enters turbine components, such as the blade outer air seals and airfoils. The specifics of the louver design are illustrated in Figure 2. The objective of the louver design is to direct particles to a downstream collector while passing particle-free flow through the louver passages. As can be seen there are several parameters that can be evaluated to achieve good particle collection with minimal pressure losses. These parameters include louver gap, length, angle, and shape. Louver shapes considered include straight, bent-tip, concave, and convex surfaces.

The design space considered for the overall louver design was held constant throughout this study as shown in Figure 2a. This constraint required that some of the louver parameters remain constant. The louver array angle, θ, was held constant, but louver gap and length were varied, as shown in Figure 2b and summarized in Table 1. Previous studies [16,18,19] have shown the effects of louver length and spacing on particle separation and pressure loss.

Table 2 shows the range of values for the louver parameters investigated over the course of the current study.

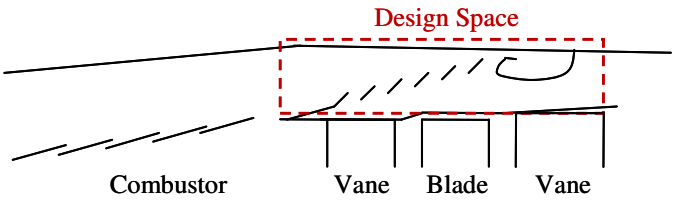

Figure 1. The separator is located within the engine in an empty cavity downstream of the combustor.

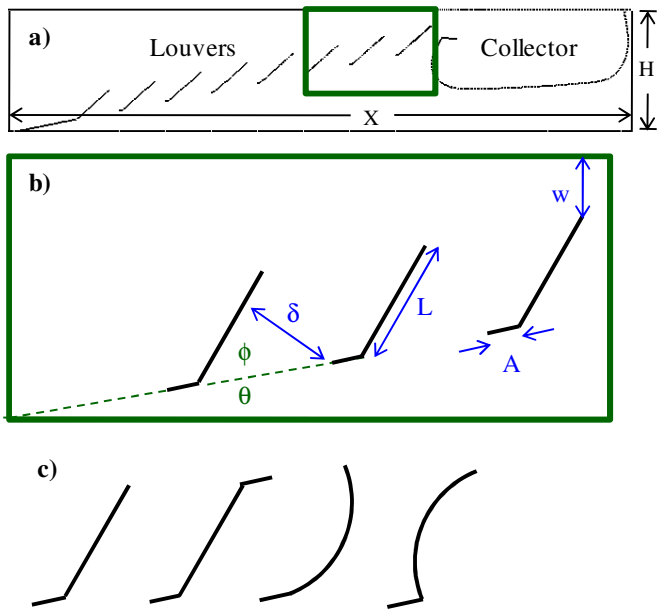

Figure 2. Drawing showing the a) separator design space, b) primary louver parameters, and c) louver shapes including straight, bent tip, concave, and convex.

Table 1. Result of Changing Separator Parameters

Parameter	Change	Affected Parameter	Effect
Number of Louvers	↑	Louver Gap, δ	↓
Area Ratio, AR	↑	Louver Gap, δ	↑
Louver Angle, ϕ	↑	Louver Length, L	↓

Table 2. Parameter Range of Values

Parameter	Min	Max
Louver Angle, ϕ	30°, 45°, 60°	
Louver Gap, δ/X	0.010	0.038
Louver Length, L/X	0.012	0.075
Louver Anchor, A/L	0.021	6.449
Dimension w, w/H	0.126	0.257
Area Ratio, AR	0.5	1.50

Louver thickness was neglected during this study since it has been shown to affect separation efficiency by no more than 10% [19]. Other computational studies [17-19] have also neglected louver thickness. Furthermore, the louver length, louver gap, louver anchor length and the dimension w, shown in Figure 2b, are not controlled parameters. Instead, their values are determined from the relations presented in the nomenclature. The controlled parameters are the number of louvers, area ratio, louver angle, and louver shape. However, dimension w was required to be larger than the louver gap of the last louver row so as to not influence the area ratio of the separator.

The collector, shown in Figure 2a, has key features that were modified, including the collector inlet and the surface shape. Different overall collector shapes were investigated to find a design that trapped particles using surface deflections and by entraining particles in a favorable circulation pattern within the collector.

To design the particle separator for minimal pressure losses and good particle collection, the design parameters were independently investigated. A methodical approach was taken by considering each of the following three features of the louver separator: the area ratio, the louver geometry, and the collector design. More specifically, the best area ratio, AR, was first determined by evaluating pressure loss across the louver array until the pressure loss was reduced to its lowest value. This best area ratio was then held fixed and the most effective louver geometry without a collector was determined by evaluating collection efficiency until the collection efficiency was increased to its maximum value. The louver geometry without the collector is shown in Figure 3a. After having determined the best louver geometry and area ratio, a collector was added to the configuration, as shown in Figure 3b. An effective collector design was defined by one that increased particle collection while not significantly increasing the pressure loss. Results indicated that the pressure loss was not significantly affected by the collector and, as such, the particle collection efficiency was the focus.

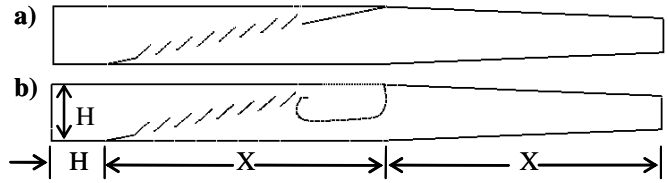

Figure 3. Two-dimensional louver model showing a) design space without collector and b) design space with collector.

COMPUTATIONAL METHODOLOGY

All computational work was performed using FLUENT 6.3.26 [21], a commercially available CFD solver, to solve for the flow field and particle trajectories. A Lagrangian particle tracking model was chosen, which uncoupled the particle trajectory calculations from the flow field calculations, similar to previous studies [11,12,14,15,18-20].

The separator flow was solved using RANS equations with the k-ω turbulence model, as well as enhanced wall functions that blend the linear and logarithmic laws of the wall. The computational domain, illustrated in Figure 3b, has upstream and downstream sections added to the design space each with axial lengths of H and X. The downstream section converges to an exit height 60% of the inlet height to remove reversed flow at the exit boundary. Temperatures in the computational domain were considered constant. Mass flow inlet and pressure outlet boundary conditions used engine matched values.

The remaining domain boundaries and separator surfaces were modeled as no-slip walls. The flow was assumed to be steady, incompressible, and an ideal gas. Flow solutions were 2^{nd} order accurate and generally took, on average, 5,000 iterations to meet the convergence criteria of 10^{-6} for all variables.

To ensure grid insensitivity, the computational grid was refined until the calculated pressure loss did not change with grid refinement. The grid was refined in regions where the local total pressure gradient was less than 10% of the maximum gradient. A grid size of approximately 45,000 cells was required for grid independent flow field results, including approximately 4,000 cells inside the collector. It was found that grid resolution in the collector affected particle trajectory calculations. The grid for the louver separator consisted of quadrilateral cells. Grid quality was evaluated by cell skewness, in which 94% of all cells had skewness less than 0.60, and an average skewness of 0.15.

The modeling of particle trajectories made use of FLUENT's discrete phase model, which calculates trajectories using flow velocity from the solved flow field. The discrete phase model is applicable when the volume ratio of particles to fluid is much less than one [22]. The discrete phase model neglects particle-particle interactions and assumes that the presence of the particles does not change the flow field. Similar to previous works [11,12,14,15,18-20], a force balance

equation, which is shown per unit mass in equation 1 [22], was used to calculate particle trajectories. The equation is reduced to only a drag force term by neglecting gravity and the term F_x. The variable F_x is an additional force term, per unit mass, that describes the force to accelerate the fluid surrounding the particle and the pressure gradient of the fluid acting on the particle. This F_x term can be neglected when the fluid to particle density ratio is much less than one [22]. In this study the ratio of fluid to particle density is on the order of 10^{-3}.

$$\frac{dU_p}{dt} = \frac{18\mu}{\rho_p d_p^{\,2}} \frac{C_D\, Re_p}{24}\left(U - U_p\right) + \frac{g\left(\rho_p - \rho_f\right)}{\rho_f} + F_x \qquad [1]$$

$$C_D = \frac{24}{Re_{sph}}\left(1 + b_1 Re_{sph}^{\,b_2}\right) + \frac{b_3 Re_{sph}}{b_4 + Re_{sph}} \qquad [2]$$

Particle trajectories were calculated from the integration of equation 1. Turbulent dispersion of particle trajectories was not accounted for; instead, mean velocity values were used in equation 1. Previous studies [11,12] using the mean velocity to calculate particle trajectories found good agreement with experimental data. The number of integration steps and length factor were chosen to be 20,000 and 6 mm, respectively. The length factor is used to determine the integration time step for solving equation 1. These values of integration steps and length factor allow sufficient calculation of particle trajectories to allow all particles not trapped in the collector to escape the domain. The domain exit was set to an escape boundary condition to allow uncollected particles to leave the domain.

Previous studies [11,12,14,15,19] have used a range of values for restitution coefficient and shape factor. Throughout this study the particles were assumed to be spherical and to have perfectly elastic impacts with the wall boundaries in the separator. Shape factor is used to modify the drag coefficient, C_D, shown in equation 2 [22], where b_n represents polynomial and exponential functions of shape factor. Restitution coefficient is used to determine the normal and tangential particle velocities after impact with a wall boundary. In this study, a value of one was used for both the restitution coefficient and shape factor. However, changes to the restitution coefficient and shape factor can slightly influence the collection efficiency results, shown in Figure 4 and Figure 5.

Figure 4 shows the dependence of collection efficiency on restitution coefficient for the best separator design found in this study, as will be described in a later section. Restitution coefficient is shown to have little effect on small particles, whereas low restitution coefficients increase collection efficiency for the large particles. An accurate restitution coefficient should be chosen based on the particle and surface materials as well as the impact angle. Previous studies [11,12,14,15] have used empirical relations taken from particle impact studies. Shape factor, defined in the nomenclature [22], is shown in Figure 5 for the best separator design found in this study. Shape factor affects small particle collection more than large particle collection because low shape factor values increase particle drag. Large particle drag influences small particle trajectories more than large particle trajectories. Large particles are not affected due to their high particle inertia, which makes them less susceptible than small particles to directional changes in the flow.

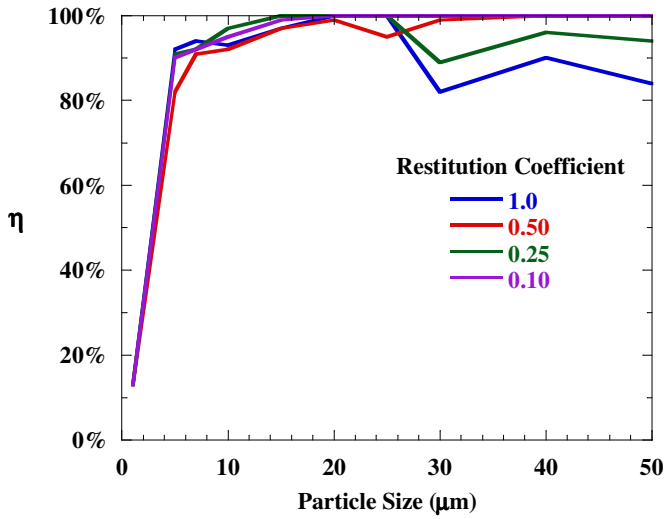

Figure 4. Effect of restitution coefficient on collection efficiency for the configuration: AR=1.50, 8 louvers, straight louvers, ϕ=30° to 45° to 30°, with collector.

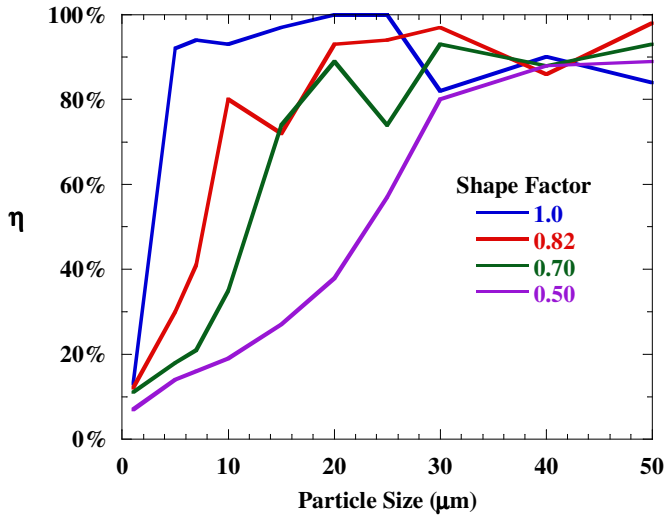

Figure 5. Effect of shape factor on collection efficiency for the configuration: AR=1.50, 8 louvers, straight louvers, ϕ=30° to 45° to 30°, with collector.

A shape factor of 0.82 is consistent with previous studies [11,15] and is shown in Figure 5 to give collection efficiency results within 20% of a shape factor value of 1.0 for most particle sizes. It must also be pointed out that previous studies [11,15] use a different equation to define shape factor. An approximated relationship between the shape factor equation used in this study and previous studies [11,15] was found to indicate a shape factor of 0.82 was consistent with the previous studies [11,15]. In addition to the shape factor dependency shown in Figure 5, overall particle collection decreases with shape factor, shown in Table 3. Overall

particle collection values are calculated by integrating the collection efficiency curves shown in Figure 5.

Table 3. Shape Factor Effect on Overall Collection

Shape Factor	1.0	0.82	0.70	0.50
Overall Collection	87%	78%	71%	54%

The particle size distribution of interest ranged from 1-50 μm. This size range makes up 75% of sand sizes found in atmosphere, as shown in Figure 6. Walsh et al. [4] found that blockage of turbine cooling channels occurs for sand with particle sizes smaller than 100 μm.

For simulations in FLUENT, ten discrete particle sizes were injected with the same number of particles per size injected, as shown in Figure 6. Each of the ten particle sizes was injected equally spaced along the inlet of the computational domain in groups of 100. The number of particles injected was determined to be sufficient for collection efficiency results to be independent of the number of injected particles.

Particle trajectories predicted by FLUENT were checked using the Stokes number, which is a dimensionless ratio of particle reaction time, τ_{rea}, to residence time, τ_{res} [24]. A Stokes number much less than one indicates that the particle will follow the flow field and a value much greater than one indicates that the particle will deviate from the flow. Stokes numbers were calculated for various particle sizes along their trajectories, particularly near the louvers. Stokes number predictions of whether or not particles separated from the flow direction were found to be consistent with the computational predictions.

Collection efficiency, η, was used as the variable to define how successful the louver separator removed particles from the flow. The efficiency, defined in the nomenclature, is calculated from the number of particles injected at the domain inlet and the number of particles that escape the domain exit. Particles that do not escape the domain exit were assumed to be collected. This differs from the reviewed numerical studies [11,12,14,15,18,19] that base separation efficiency on mass rather than on number of particles.

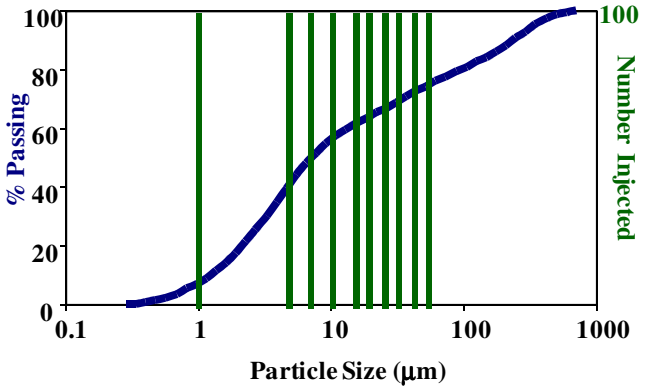

Figure 6. Size distribution of particles used in the computational domain representing those of interest [23].

In this study the efficiency was determined for each particle diameter injected. As such, the collection efficiency reported in this study is for a given particle size. Pressure loss across the separator was evaluated by integrating mass-weighted total pressure values at the inlet and exit of the computational domain.

DISCUSSION OF RESULTS

A methodical approach was used in evaluating three primary components of the separator: the area ratio; the louver design; and the collector design. The inlet Reynolds number remained constant for all studies at 135,500. Pressure loss and collection efficiency predictions were considered for all calculations. The next sections of the paper present a summary of what was learned for each of the steps. Results of previous studies [11,15] have shown that small particles (less than 7μm) were more difficult to separate from the flowstream than large particles (greater than 40μm). Our study agreed with those findings. In this paper, particles less than 7μm are considered small particles and particles greater than 40μm are considered large particles. The focus in designing the area ratio and louver geometry was to increase the collection of small particles, whereas the focus for the collector design was to increase the collection of large particles.

Selection of the Area Ratio

The best area ratio for the separator was determined using an initial louver geometry of straight louvers with ϕ=30° for different numbers of louvers. The focus was to ensure particle collection while minimizing the pressure loss.

Figure 7 shows that increasing the area ratio from 0.50 to 1.50 decreases the pressure loss by approximately 0.5%. The reduction of flow restriction through the louvers causes the decrease in pressure loss. Although area ratios of 1.25 and 1.50 result in the lowest pressure loss through the array, the predicted pressure losses of all of the area ratios is considered to be insignificant to overall engine performance.

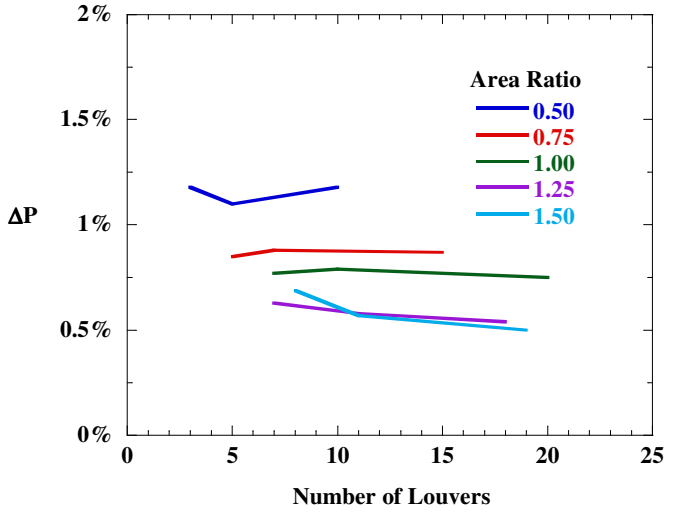

Figure 7. Pressure loss is shown to decrease with increasing area ratio for configurations with straight louvers at ϕ=30°, without collector.

With respect to the collection efficiency, Figure 8 indicates the efficiency for each particle diameter for 1.25 and 1.50 area ratios. Each of the two area ratios has a different number of louvers. Figure 8 shows both area ratios have better small particle collection with fewer louvers, and better large particle collection with many louvers. Each louver is longer for a configuration with few louvers compared to a configuration with many louvers. The relationship between louver length and the particle sizes collected will be described in more detail in the following section.

An area ratio of 1.50 was chosen for the remainder of the study because it resulted in low pressure loss and high small particle collection. Compared to the other parameters that were investigated (louver shape and collector geometry), the area ratio was found to have the largest effect on pressure loss. Therefore, the remainder of the study focused on particle collection without attempting to further reduce the pressure losses.

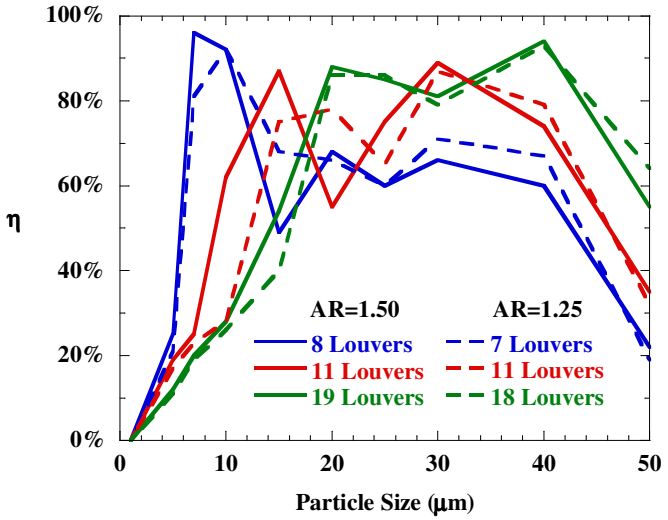

Figure 8. Collection efficiency for area ratios of 1.25 and 1.50, straight louvers at ϕ=30°, without collector.

Design of the Louvers

The area ratio investigation performed in this study confirmed from previous studies [11,15] that trajectories for small particles (less than 7μm) were dominated by their reaction to the local flow field in comparison to trajectories for large particles (greater than 40μm). It was also seen that large particles were easily separated such that they were directed to the region where the collector was to be placed. However, small particles, due to their small inertia, were shown to be difficult to separate. Because of the difficulty in separating small particles, the geometry of the louver array was designed to increase small particle collection. All louver geometries investigated considered the area ratio of 1.50. Three different numbers of louvers including 8, 11, and 19 were investigated where each number resulted in a different louver gap and louver length. Comparisons of simulation results using a baseline configuration of 11 louvers were made between more than 20 unique configurations. Louver geometries with the best performance were further evaluated in an array containing 8 and 19 louvers.

Collection efficiency was predicted to be dependent on the number of louvers as well as the louver angle and shape. Pressure loss was not significantly affected by the louver geometry. Figure 8 shows that small particle collection efficiency is greater when a small number of louvers are used, compared to a large number of louvers. Adversely, small particle collection is predicted to decrease as the louver angle is increased, as shown in Figure 9. In addition, small particle collection is also predicted to decrease for concave or convex louvers as shown in Figure 9.

Recall, Figure 2 illustrates the convex and concave louver geometry. Increasing the louver angle and using concave or convex louvers decreases the collection of small particles because these changes decrease the length of the louvers. A larger number of louvers in the configuration also decrease the length of each louver.

Long louvers cause an increase in flow velocity and particle momentum by converging the flow since the top domain wall remains fixed. The high momentum results in the small particles being less susceptible to directional changes of the flow and bypassing the louver passages, as illustrated in Figure 10. Large particle collection is shown to decrease with increased louver lengths. Increasing the large particle momentum beyond the already high value causes the tendency for large particles to have many deflections from the separator walls and louvers. As such, the large particles ultimately pass through the last louver passage, as shown in Figure 11.

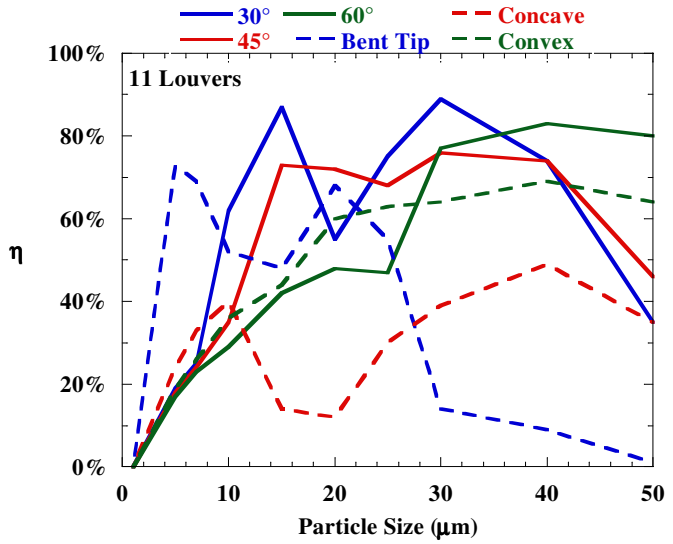

Figure 9. Collection efficiency for varying louver angle and shape, AR=1.50, without collector.

Bent tip louvers, also illustrated in Figure 2, were shown to increase small particle collection over straight louvers, as shown in Figure 9. This increase in collection occurs because the louver length of the bent tip louvers is comparable to straight louvers, while additionally reducing the effective flow area between louvers. The reduction in effective flow area causes an abrupt change in flow direction around the louvers, allowing the momentum of the small particles to carry the particles away from the louver passages as shown in Figure 12. This effect has also been found by Poulton et al. [19]

where the reduction in flow area was caused by the separation region behind straight louvers.

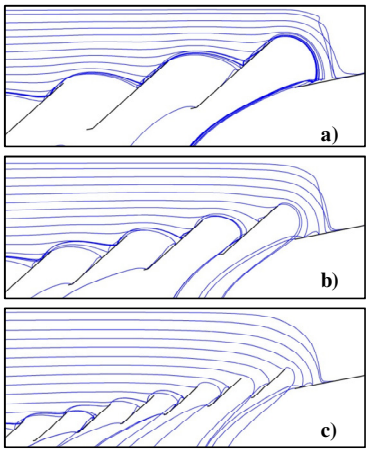

Figure 10. Particle trajectories for 5μm particles, showing an increase of curvature with louver length for AR=1.50, ϕ=30° configurations, without collector, with a) 8, b) 11, and c) 19 louvers.

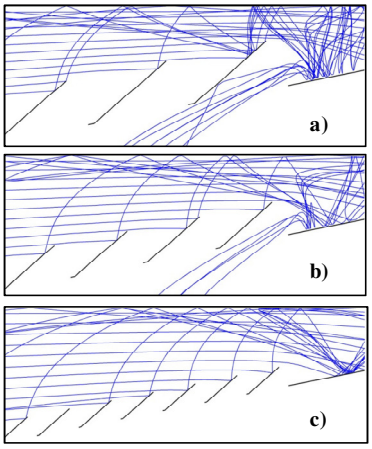

Figure 11. Particle trajectories for 40μm particles, showing increasing surface deflections with increased louver lengths for AR=1.50, ϕ=30° configurations, without collector, with a) 8, b) 11, and c) 19 louvers.

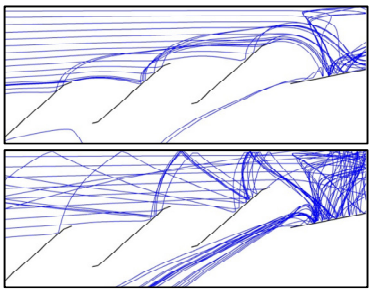

Figure 12. Particle trajectories through an 8 louver, AR=1.50, bent tip ϕ=30° louver configuration, without collector, for 5μm (upper) and 40 μm (lower) particle sizes.

Investigations were also carried out by varying the louver geometry along the louver array by changing individual louvers. Results from representative configurations are shown in Figure 13 with 8 louvers in each configuration. Louver angles are varied along the array by incrementally changing the louver angle, such as configuration B. Configuration B varies the louver angle from ϕ = 60° to 30° and was predicted to perform slightly better than the baseline ϕ = 30° configuration (configuration A). Furthermore, some louver configurations combine both straight and bent tip louvers. It was thought that the success of the bent tip louver would be additive to the success of the straight louver configurations. Figure 13 shows that combining the bent tip and straight louvers into one configuration (configuration D) does not result in better performance than either louver configuration alone. Figure 13 shows the best performing louver configuration was found to have straight louvers at varying angle from ϕ = 30° to 45° to 30° uniformly incremented along the 8 louver array. The best design geometry is shown in Figure 14. Eight louvers were chosen for the best design because, as explained earlier, fewer louvers in the configuration result in higher small particle collection. Although the best design (configuration E) shown in Figure 13 has low efficiency in collecting large particles, the collector itself still needed to be modified to improve the large particle collection.

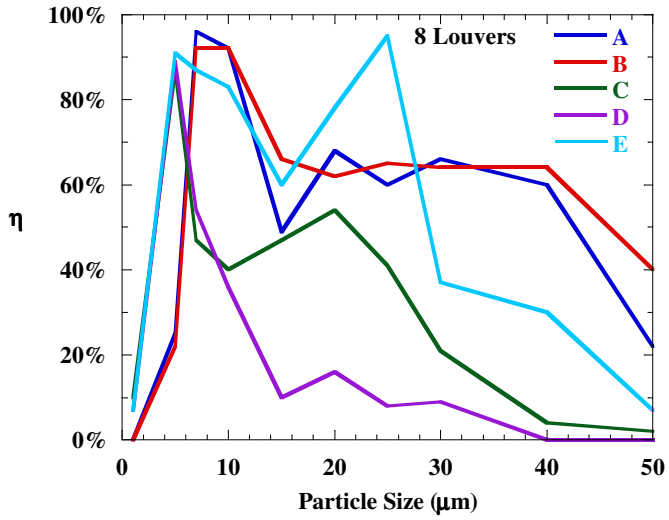

configuration A	30°, straight louvers
configuration B	60° - 30°, straight louvers
configuration C	30°, all bent tips
configuration D	60° - 30°, bent last three tips
configuration E	30°- 45°- 30°, straight louvers

Figure 13. Collection efficiency is affected by varying louver angle and louver shape along the louver array.

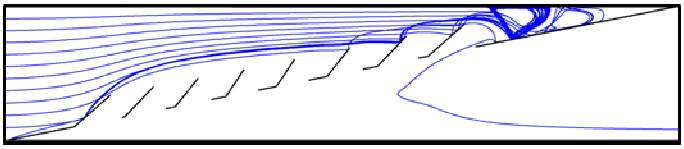

Figure 14. The best performing louver configuration varies the louver angle from ϕ = 30° to 45° to 30° along the array, resulting in higher small particle collection with 5μm particles shown.

Design of the Collector

The remainder of the study focused on the design of the collector using the previously determined area ratio of 1.50 and the louver configuration of 8 louvers with varying louver angle from ϕ = 30° to 45° to 30° along the array, as shown in Figure 14. The purpose of the collector is to provide a place for particles to remain after they have been separated from the flow. In the actual gas turbine application, this collector will need to be cleaned periodically to remove the collected particles. The collector design focused on increasing large particle collection with the goal that the small particle collection should not decrease.

The contour shape of the collector walls and the collector inlet were modified and the effects are shown in Figure 15. Curved collector walls show better large particle collection than straight walls with no apparent reduction of small particle collection. The straight wall designs that were investigated were not able to reflect the large particles such that they remained in the collector.

To improve the large particle collection, it is desirable to have a collector inlet section to restrict particles from leaving the collector after having been captured. It was found that a lip added to the collector inlet helped to deflect particles away from the collector inlet and keep them within the collector region. Predictions also indicate that the lip created an inlet vortex, as shown in the upper image of Figure 16. The louver geometry also helps to establish this vortex by increasing the flow velocity passing over the last louver tip. If the louver exit velocity is not large enough, the flow will not impinge on the inlet lip in such a way to develop the vortex as shown in the lower image of Figure 16.

Figure 15 indicates the improved collection efficiency when a lip with a vortex at the inlet to the collector is present. The circulation direction of the vortex is essential to set up a favorable circulation pattern within the collector. Figure 16 compares circulation patterns with and without a vortex at the inlet to the collector. The favorable circulation pattern set up in the collector results in particle trajectories that are not directed back towards the collector inlet. Figure 17 shows representative particle paths for 40μm and 5μm particles for the best design configuration that has the favorable collector circulation. Alternatively, without the inlet vortex, particles are directed towards the inlet by the unfavorable circulation, thereby exiting the collector.

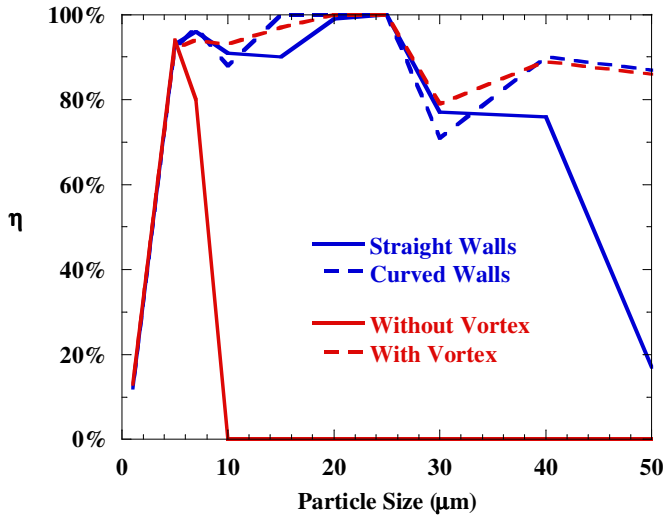

Figure 15. Key geometry features of the collector are shown to affect collection efficiency for the configuration: AR=1.50, 8 louvers, straight louvers, ϕ = 30° to 45° to 30°.

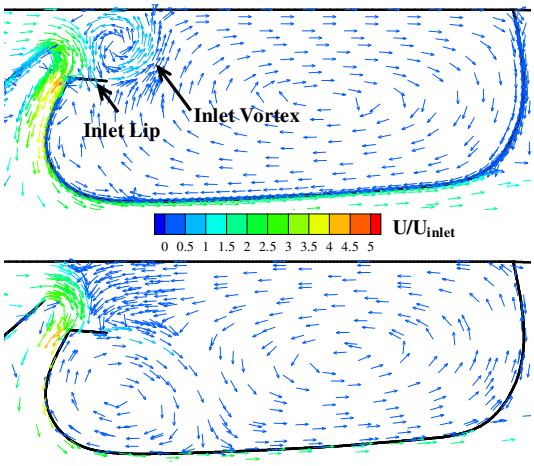

Figure 16. Collector circulation patterns showing (upper) clockwise rotation with an inlet vortex, and (lower) counter-clockwise circulation without an inlet vortex.

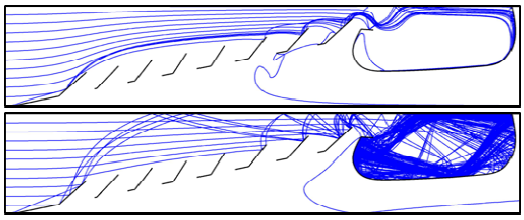

Figure 17. Particle trajectory plot showing the collecting pattern for 5μm (upper) and 40μm (lower) particles in the best separator design.

CONCLUSIONS

A methodical design of an inertial particle separator that does not utilize scavenge flow to aid particle separation has been presented. The separator is intended for placement downstream of the combustor section of a gas turbine. The successful design removes particles from the coolant stream and traps the particles in a static collector that can be periodically cleaned. The separator consisted of an array of louvers followed by a static collector.

The results indicated that the pressure losses across the separator louver array were primarily dictated by the flow area ratio. An area ratio of 1.50 was found to have minimal (< 1%) impact on the overall engine performance in terms of pressure losses. Predicted results for an area ratio of 1.50 indicated that particle diameters less than 7μm were better collected with a smaller number of louvers than a larger number of louvers. The design of the louver geometry indicated that small particle collection was increased for louver configurations with long louver lengths. Straight louvers at varying louver angles were found to have better collection than curved louvers or bent tip louvers. Predicted results indicated that varying the angle of straight louvers along the louver array resulted in better collection efficiency compared to a constant louver angle.

To collect the separated particles, a collector was designed to trap particles by entraining them in a clockwise fluid rotation. The geometric features that were important for the collector included curved walls and a lip placed at the inlet to the collector. The key flow feature that was found to best collect the particles was the presence of an inlet vortex, caused by flow impinging on the collector inlet lip. This vortex at the inlet to the collector was found necessary to set up a favorable circulation pattern in the collector. The circulation pattern directed particle trajectories away from the collector inlet so the particles could not escape. The vortex phenomenon was important because it can be utilized in the design of any device that requires particles having a range of sizes to be separated from the working fluid where a scavenge flow is not possible.

ACKNOWLEDGMENTS

The authors would like to thank Pratt & Whitney for funding and sponsoring this research effort including Joel Wagner, Ryan Levy, and Takao Fukuda.

REFERENCES

[1] Moroianu, D., Karlsson, A., Fuchs, L., 2004, "LES of the Flow and Particle Ingestion into an Air Intake of a Jet Engine Running on the Ground," GT2004-53762.

[2] Hamed, A., Tabakoff, W., 2006, "Erosion and Deposition in Turbomachinery," *J. Propulsion and Power*, **22** (2), pp. 350-360.

[3] Land, C.L., Thole, K.A., Joe, C., 2008, "Considerations of a Double Wall Cooling Design to Reduce Sand Blockage," GT2008-50160.

[4] Walsh, W.S., Thole, K.A., Joe, C., "Effects of Sand Ingestion on the Blockage of Film-Cooling Holes," International Gas Turbine and Aeroengine Congress and Exposition, Barcelona, Spain, ASME Paper GT2006-90067.

[5] Cardwell, N.D., Thole, K.A., Burd, S.W., 2008, "Investigation of Sand Blocking Within Impingement and Film-Cooling Holes," GT2008-51351.

[6] Schneider, O., Dohmen, H.J., Reichert, A.W., 2002, "Experimental Analysis of Dust Separation in the Internal Cooling Air System of Gas Turbines," GT2002-30240.

[7] Schneider, O., Dohmen, H.J., Benra, F.-K., Brillert, D., 2003, "Investigations of Dust Separation in the Internal Cooling Air System of Gas Turbines," GT2003-38293.

[8] Schneider, O., Dohmen, H.J., Benra, F.-K., Brillert, D., 2004, "Dust Separation in a Gas Turbine Pre-Swirl Cooling Air System, a Parameter Variation," GT2004-53048.

[9] Schneider, O., Benra, F.-K., Dohmen, H.J., Jarzombek, K., 2005, "A Contribution to the Abrassive Effect of Particles in a Gas Turbine Pre-Swirl Cooling Air System," GT2005-68188.

[10] Syred, C., Griffiths, A., Syred, N., 2004, "Gas Turbine combustor with Integrated Ash Removal for Fine Particulates," GT2004-53270.

[11] Breitman, D.S., Duek, E.G., Habashi, W.G., 1985, "Analysis of a Split-Flow Inertial Particle Separator by Finite Elements," *J. Aircraft*, **22** (2), pp 135-140.

[12] Vittal, B.V.R., Tipton, D.L., Bennett, W.A., 1985, "Development of an Advanced Vaneless Inlet Particle Separator for Helicopter Engines," AIAA/SAE/ASME/ASEE 21st Joint Propulsion Conference.

[13] Shieh, C.F., Delaney, R.A., 1984, "Analysis of the Flow Field in an Engine Inlet Particle Separator," *ASME Fluids Engineering Division* (Publication), **14**, pp 23-28.

[14] Zedan, M., Mostafa, A., Hartman, P., 1992, "Viscous Flow Analysis of Advanced Particle Separators," *J. Propulsion and Power*, **8** (4), pp 843-848.

[15] Ghenaiet, A., Tan, S.C., 2004, "Numerical Study of an Inlet Particle Separator," GT2004-54168.

[16] Zverev, N.I., 1946, "Shutter-Type Dust Collector of Small Dimensions," *Engineer's Digest*, **7** (11), pp. 353-355.

[17] Smith, Jr., J.L., Goglia, M.J., 1956, "Mechanism of Separation in Louver-Type Dust Separator," *ASME Transactions*, **78** (2), pp. 389-399.

[18] Gee, D.E., Cole, B.N., 1969, "A Study of the Performance of Inertia Air Filters," *Inst. Mech. Engineers - Symposium on Fluid Mechanics and Measurements in Two-Phase Systems, University of Leeds*, pp. 167-176.

[19] Poulton, P., Cole, B.N., 1981, "An Experimental and Numerical Investigation of Louvred Inertia Air Filter Performance," *Conference on Gas Born Particles, Institution of Mechanical Engineers*, pp. 161-170.

[20] Jones, G.J., Mobbs, F.R., Cole, B.N., 1971, "Development of a Theoretical Model for an Inertial Filter," *Pneumotransport 1 – 1st Int'l. Conf. on Pneumatic Transport of Solids in Pipes*, Paper B1.

[21] ANSYS, Inc., Version 6.3.26, 2008 (ANSYS Inc.: New Hampshire)
[22] Fluent User Guide, ANSYS, Inc., Version 6.3, 2008 (ANSYS, Inc.: New Hampshire).
[23] Particle size distribution provided by Pratt & Whitney, 2007.
[24] Schetz, J., Fuhs, A., 1996, *Handbook of Fluid Dynamics and Fluid Machinery*, Vol 1, John Wiley & Sons, Inc., New York, pp 905-906, Chap. 14.